Electronic Supplementary Material (ESI) for New Journal of Chemistry.
This journal is © The Royal Society of Chemistry and the Centre National de la Recherche Scientifique 2023

Electronic Supplementary Material (ESI)

Two novel metal-organic frameworks constructed by pyridinyl-derived and carboxylate mixed ligands for photocatalytic dye degradation

Chixiao Ma [a,c], Junyong Zhang,*[a] Hao Xu,[a] Xianghua Zeng,[a] Chunhua Gong*[b] and Jingli Xie*[a]

Supplementary Figures and Tables.

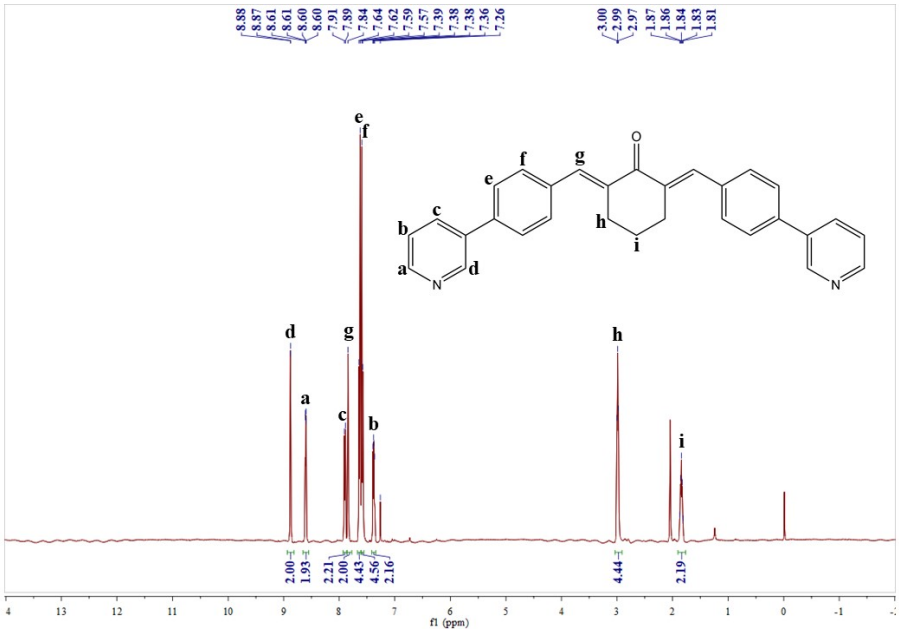

(a)

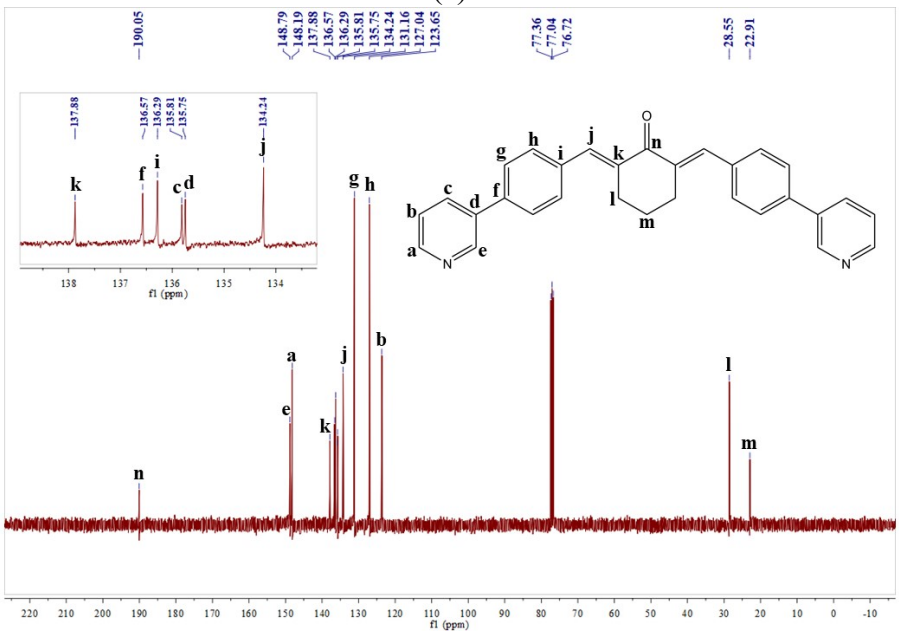

(b)

Fig. S1 (a) ^{1}H NMR spectrum of **L**. (b) ^{13}C NMR spectrum of **L**.

Table S1 Crystallographic data for **L**, **1** and **2**.

Compound	**L**	**1**	**2**
Empirical formula	$C_{30}H_{24}N_2O$	$C_{39}H_{30}ZnN_2O_5$	$C_{39}H_{30}CdN_2O_5$
Formula weight	428.51	672.02	719.05
Temperature (K)	296(2)	296(2)	296(2)
Crystal system	Monoclinic	Triclinic	Triclinic
Space group	$P2_1/c$	$P\bar{1}$	$P\bar{1}$
a (Å)	10.3942(4)	9.1906(8)	9.2944(6)
b (Å)	8.7315(4)	9.9930(8)	10.2181(4)
c (Å)	24.6346(10)	17.5968(15)	17.8346(8)
α (°)	90	100.867(7)	74.259(4)
β (°)	101.023(4)	91.850(7)	87.391(4)
γ (°)	90	105.456(7)	73.980(5)
V (Å^3)	2194.51(16)	1523.9(2)	1566.15(15)
Z	4	2	2
D_c (g·cm^{-3})	1.297	1.465	1.525
μ (mm^{-1})	0.613	0.857	0.747
F (000)	904.0	696.0	732.0
Radiation	Cu-$K\alpha$ (λ = 1.54184 Å)	Mo-$K\alpha$ (λ = 0.71073 Å)	Mo-$K\alpha$ (λ = 0.71073 Å)
Reflections collected	7733	13116	13318
Independent reflections	4239	7113	7229
R_{int}	0.0276	0.0805	0.0504
GOF on F^2	1.021	0.827	0.854
R_1/wR_2 [$(I > 2\sigma(I)$]	0.0467/0.1141	0.0585/0.0693	0.0490/0.0538
R_1/wR_2 (all data)	0.0742/0.1296	0.1750/0.1091	0.1048/0.0616

Table S2 Selected bond lengths (Å) and angles (°) for compound **1**

Compound **1**			
Zn1-N2	2.162(4)	Zn1-N1^{iii}	2.174(4)
Zn1-O2	2.012(3)	Zn1-O3^{i}	2.040(3)
Zn1-O4^{ii}	2.081(3)	Zn1-O5^{ii}	2.363(4)
N1^{iii}-Zn1-O5^{ii}	87.17(14)	N2-Zn1-O5^{ii}	89.35(14)
N2-Zn1-N1^{iii}	172.02(16)	O2-Zn1-N1^{iii}	85.20(13)
O2-Zn1-N2	87.77(13)	O2-Zn1-O3^{i}	120.60(13)
O2-Zn1-O4^{ii}	151.03(14)	O2-Zn1-O5^{ii}	92.51(12)
O3^{i}-Zn1-N1^{iii}	91.34(15)	O3^{i}-Zn1-N2	95.51(15)

$O3^{i}$-Zn1-$O4^{ii}$	88.34(13)	$O3^{i}$-Zn1-$O5^{ii}$	146.63(12)
$O4^{ii}$-Zn1-$N1^{iii}$	93.53(14)	$O4^{ii}$-Zn1-N2	90.78(13)
$O4^{ii}$-Zn1-$O5^{ii}$	58.53(12)		

Symmetry codes: (i) 1-*x*, -*y*, 2-*z*; (ii) *x*, 1+*y*, *z*; (iii) *x*-1, *y*-1, 1+*z*.

Table S3 Selected bond lengths (Å) and angles (°) for compound **2**.

Compound **2**			
Cd1-$N1^{ii}$	2.351(3)	Cd1-N2	2.328(3)
Cd1-O2	2.243(2)	Cd1-$O3^{iii}$	2.256(3)
Cd1-$O4^{i}$	2.3296(19)	Cd1-$O5^{i}$	2.376(2)
$N1^{ii}$-Cd1-$O5^{i}$	90.21(9)	N2-Cd1-$O5^{i}$	91.90(9)
N2-Cd1-$N1^{ii}$	171.61(9)	N2-Cd1-$O4^{i}$	88.64(9)
O2-Cd1-$N1^{ii}$	85.16(9)	O2-Cd1-N2	86.73(9)
O2-Cd1-$O3^{iii}$	130.03(8)	O2-Cd1-$O4^{i}$	144.55(9)
O2-Cd1-$O5^{i}$	89.64(8)	$O3^{iii}$-Cd1-$N1^{ii}$	92.58(10)
$O3^{iii}$-Cd1-N2	90.97(10)	$O3^{iii}$-Cd1-$O4^{i}$	85.13(8)
$O3^{iii}$-Cd1-$O5^{i}$	140.33(8)	$O4^{i}$-Cd1-$N1^{ii}$	99.23(9)
$O4^{i}$-Cd1-$O5^{i}$	58.53(12)		

Symmetry codes: (i) *x*, *y*-1, *z*; (ii) *x*-1, 1+*y*, 1+*z*; (iii) 1-*x*, 2-*y*, 2-*z*;

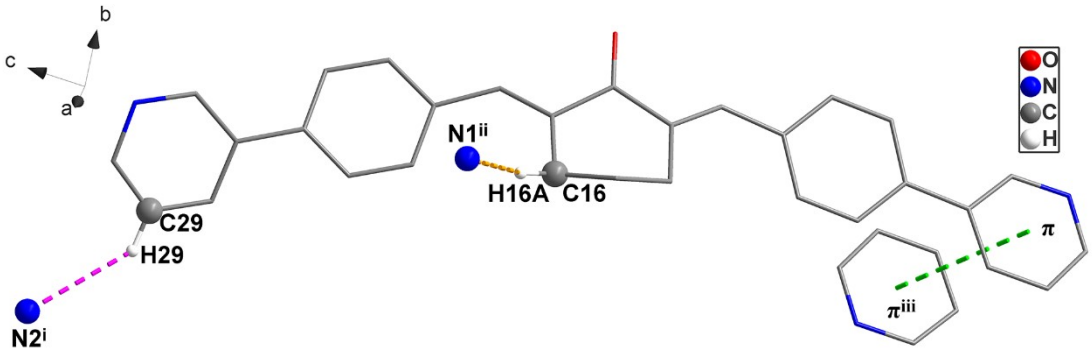

Fig. S2 Hydrogen bonding interactions in **L**.

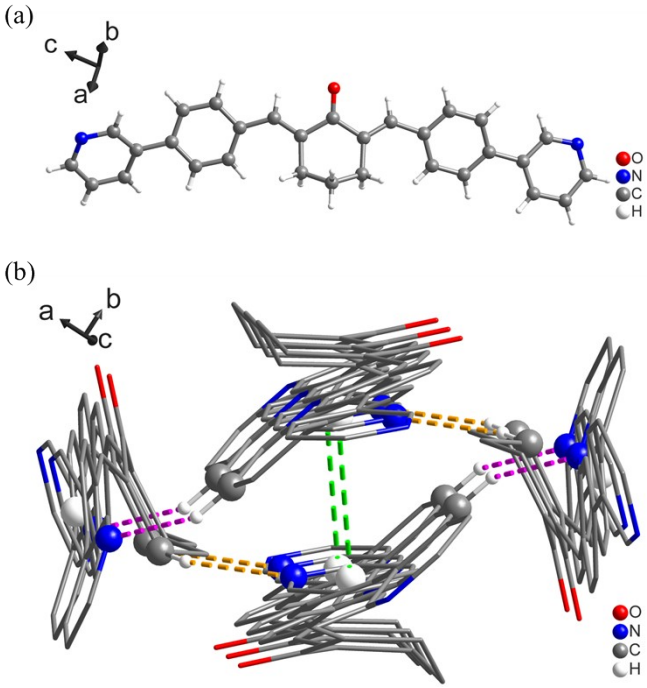

Fig. S3 (a) The structure of **L**. (b) The packing mode of **L** by hydrogen bonding interactions.

Table S4 The hydrogen-bonding geometry (Å, °) of **L**.

D–H···A	d(D–H)	d(H···A)	d(D···A)	∠D–H···A
C29–H29···N2^{i}	0.93	2.74	3.48(2)	137
C16–H16A···N1^{ii}	0.97	2.57	3.48(2)	156

Symmetry codes: (i) 2-*x*, *y*-1/2, 3/2-*z*; (ii) 1+*x*, 3/2-*y*, 1/2+*z*.

Table S5 The $\pi\cdots\pi$ interactions (Å, °) for the **L**.

Compound	$\pi\cdots\pi$ interaction	cent···cent (Å)	dihedral angle (°)
L	π(Py)···π(Py)^{iii}	3.90	0

Symmetry codes: (iii) -*x*, 1-*y*, -*z*.

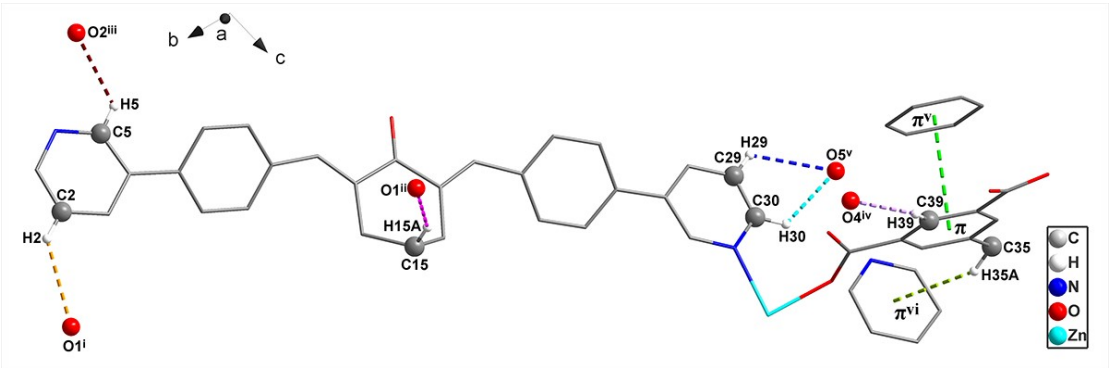

Fig. S4 Hydrogen bonding interactions in **1**.

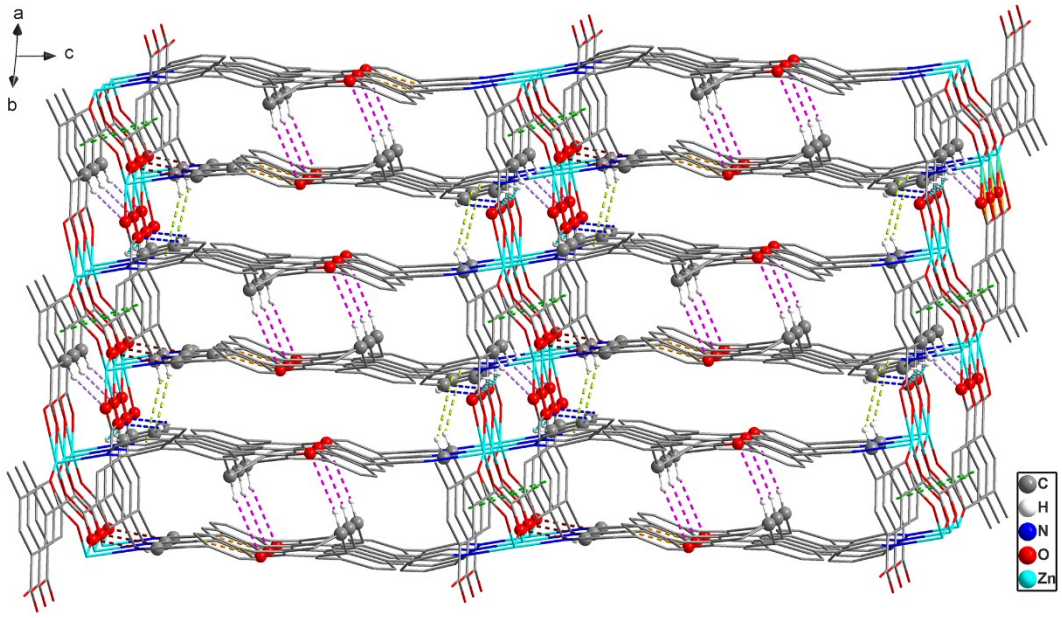

Fig. S5 3D supramolecular framework of **1** formed by the weak interactions.

Table S6 The hydrogen-bonding geometry (Å, °) of compound **1**.

D–H···A	d(D–H)	d(H···A)	d(D···A)	∠D–H···A
C2–H2···O1^{i}	0.93	2.55	3.21(2)	128
C15–H15···O1^{ii}	0.97	2.71	3.58(4)	149
C5–H5···O2^{iii}	0.93	2.31	2.88(3)	120
C39–H39···O4^{iv}	0.93	2.70	3.60(4)	162
C29–H29···O5^{v}	0.93	2.62	3.23(2)	123
C30–H30···O5^{v}	0.93	2.61	3.24(3)	125
C35–H35A···π(Ph)^{vi}	0.96	2.99	3.86(5)	150

Symmetry codes: (i) 1+*x*, 1+*y*, *z*; (ii) 2-*x*, 1-*y*, 1-*z*; (iii) 1+*x*, 1+*y*, *z*-1; (iv) 1-*x*, -1-*y*, 2-*z*; (v) -*x*, -1-*y*, 2-*z*; (vi) -*x*, -*y*, 2-*z*.

Table S7 The $\pi\cdots\pi$ interactions (Å, °) for compound **1**.

Compound	$\pi\cdots\pi$ interaction	cent···cent (Å)	dihedral angle (°)
1	π(Ph)···π(Ph)^{v}	3.61	0

Symmetry codes: (v) -*x*, -1-*y*, 2-*z*.

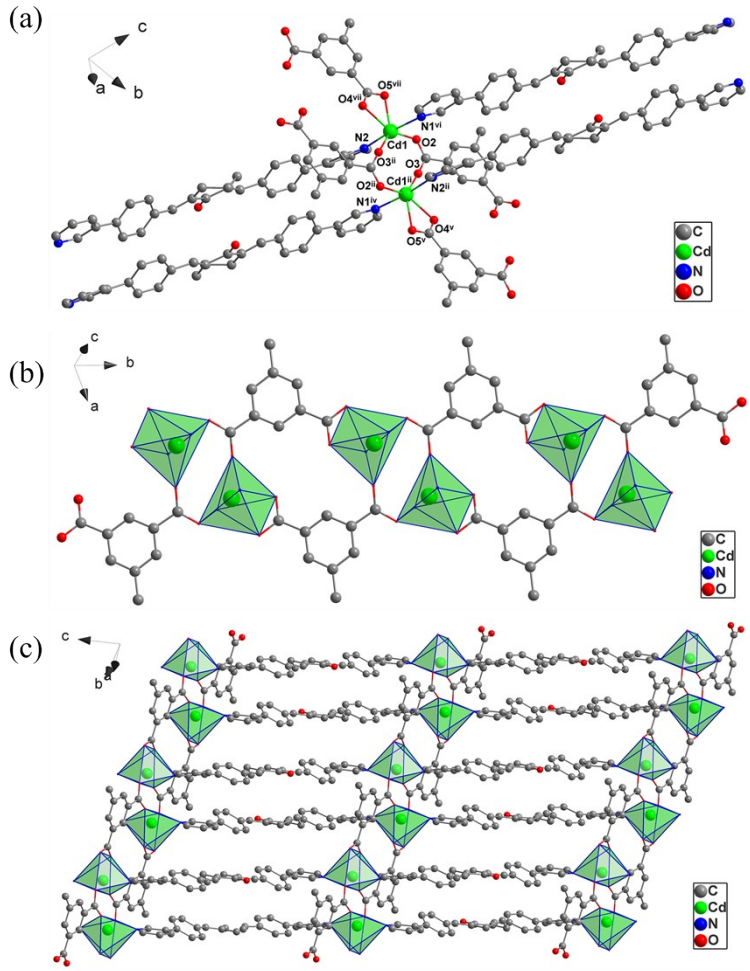

Fig. S6 Structure of compound **2**: (a) The coordination environment of Cd^{2+} ion. (b) Trapezoidal chain. (c) 2D layer structure.

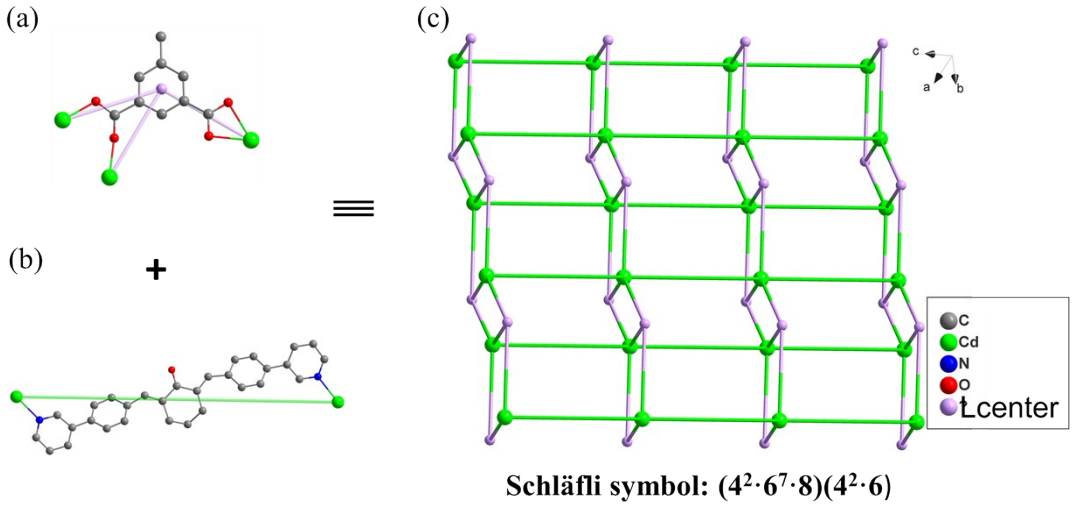

Schläfli symbol: $(4^2 \cdot 6^7 \cdot 8)(4^2 \cdot 6)$

Fig. S7 Topological simplification diagram of compound **2**.

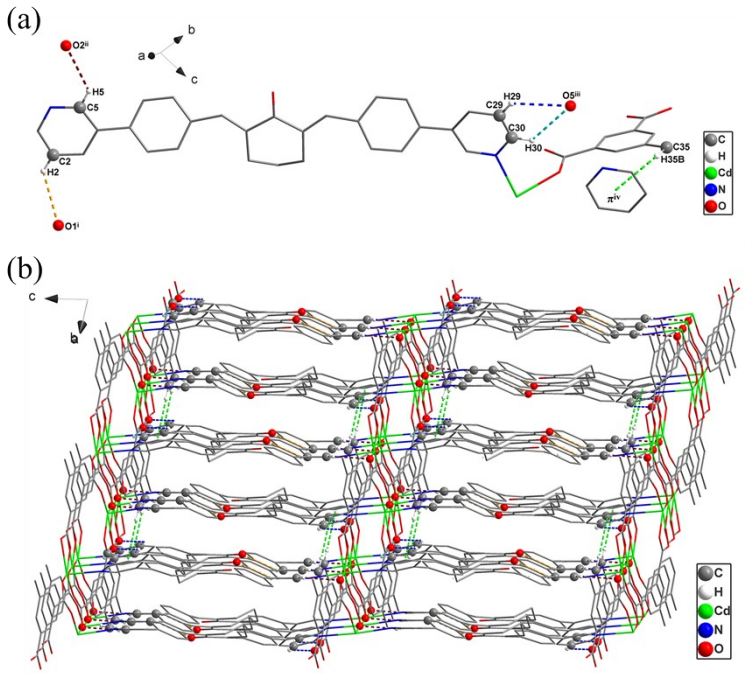

Fig. S8 (a) Hydrogen bonding interactions in **2**. (b) 3D supramolecular framework of **1** formed by the weak interactions.

Table S8 The hydrogen-bonding geometry (Å, °) of compound **2**.

D–H···A	d(D–H)	d(H···A)	d(D···A)	∠D–H···A
C2–H2···O1^{i}	0.93	2.56	3.23(5)	129
C5–H5···O2^{ii}	0.93	2.41	3.06(5)	127
C29–H29···O5^{iii}	0.93	2.70	3.32(6)	125
C30–H30···O5^{iii}	0.93	2.72	3.35(6)	125
C35–H35B···π(Py)^{vi}	0.96	3.13	4.00(6)	167

Symmetry codes: (i) 1+*x*, y-1, *z*; (ii) 1+*x*, y-1, *z*-1; iii) -*x*, 3-*y*, 2-*z*; iv) 1-*x*, -1-*y*, 2-*z*; v) -*x*, 2-*y*, 2-*z*.

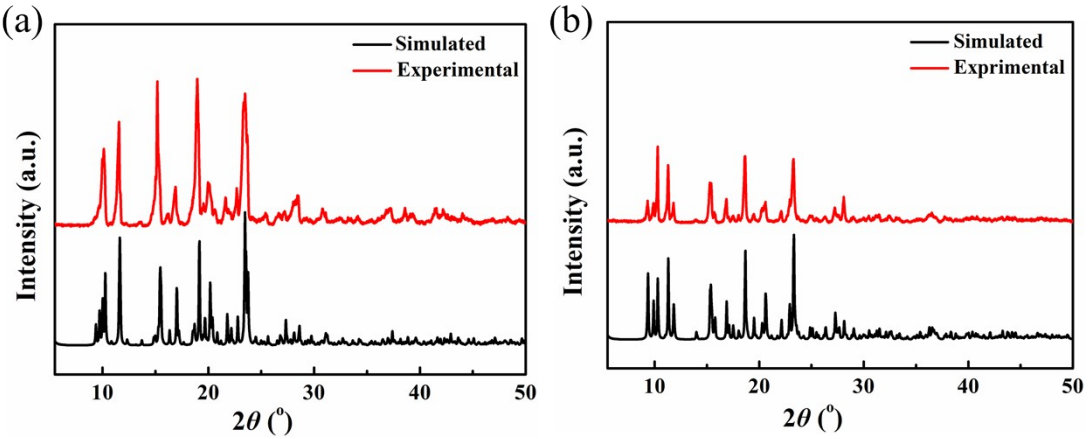

Fig. S9 (a) PXRD patterns of **1**; (b) PXRD patterns of **2**.

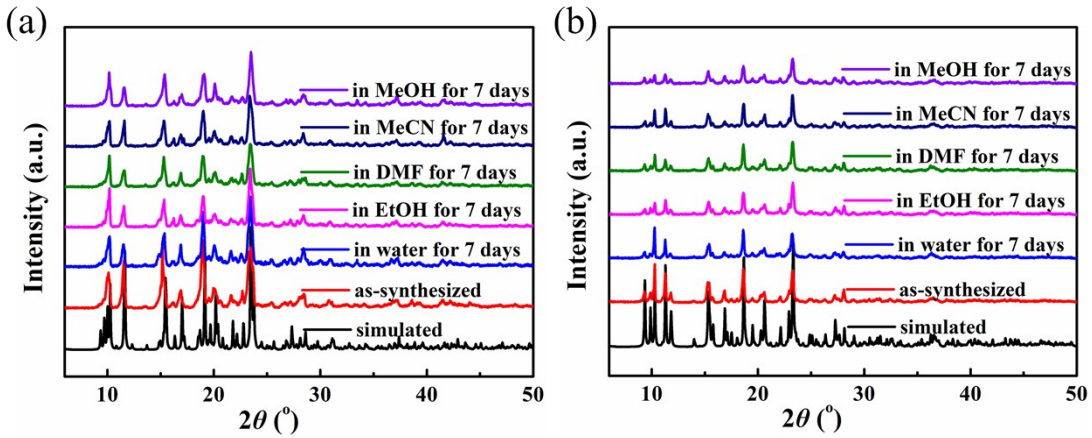

Fig. S10 (a) PXRD patterns of **1** after soaking in different solvents for a week. (b) PXRD patterns of **2** after soaking in different solvents for a week.

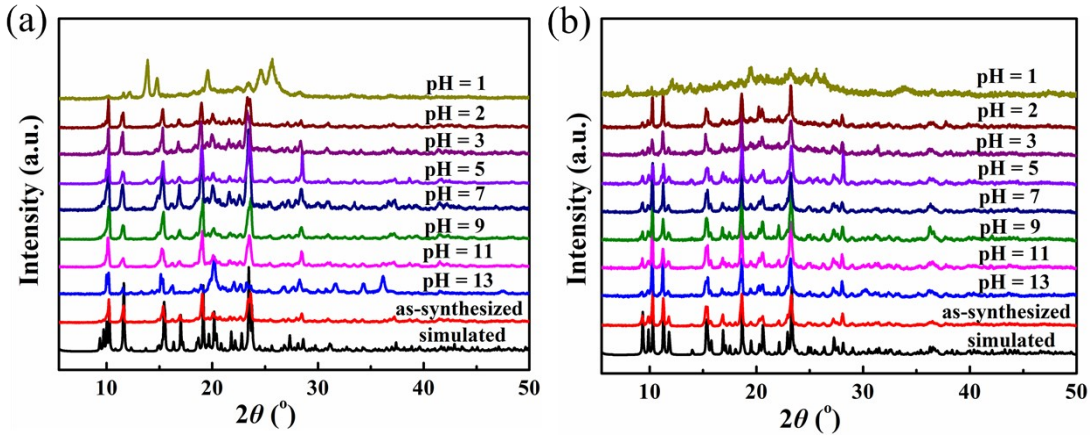

Fig. S11 (a) PXRD patterns of **1** after soaking in different pH solutions for three days. (b) PXRD patterns of **2** after soaking in different pH solutions for three days.

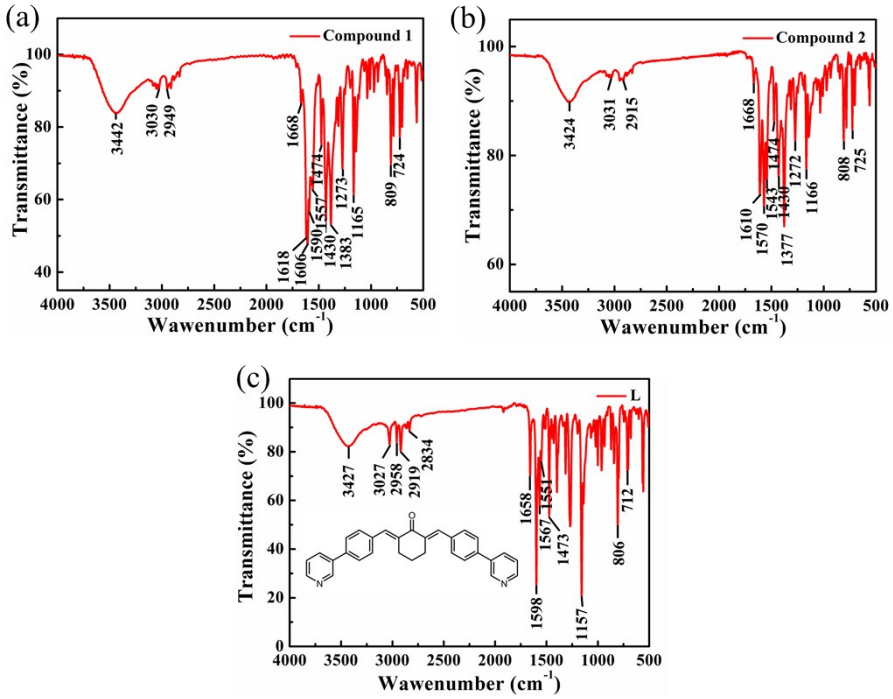

Fig. S12 (a) IR spectrum of **1**. (b) IR spectrum of **2**. (c) IR spectrum of **L**.

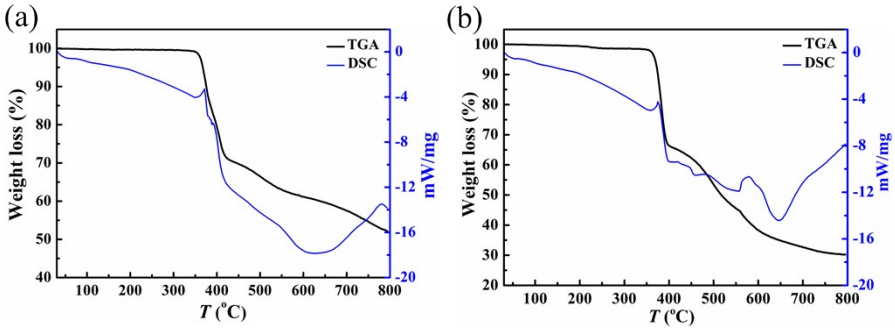

Fig. S13 (a) TG curve of **1**. (b) TG curve of **2**.

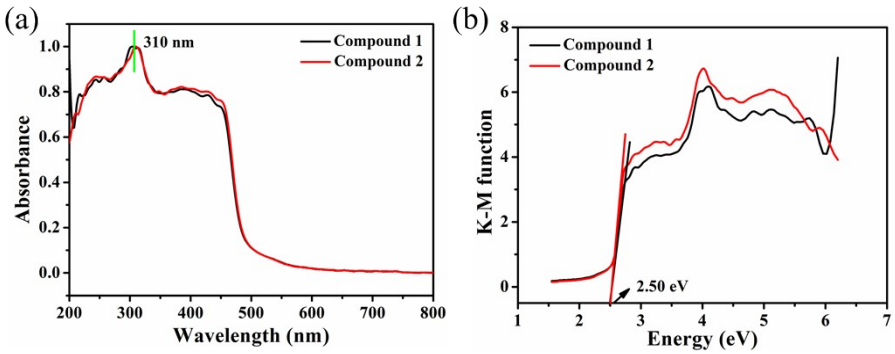

Fig. S14 (a) UV-*vis* DRS spectra of **1** and **2**. (b) Tauc plot displaying the band gap of **1** and **2**.

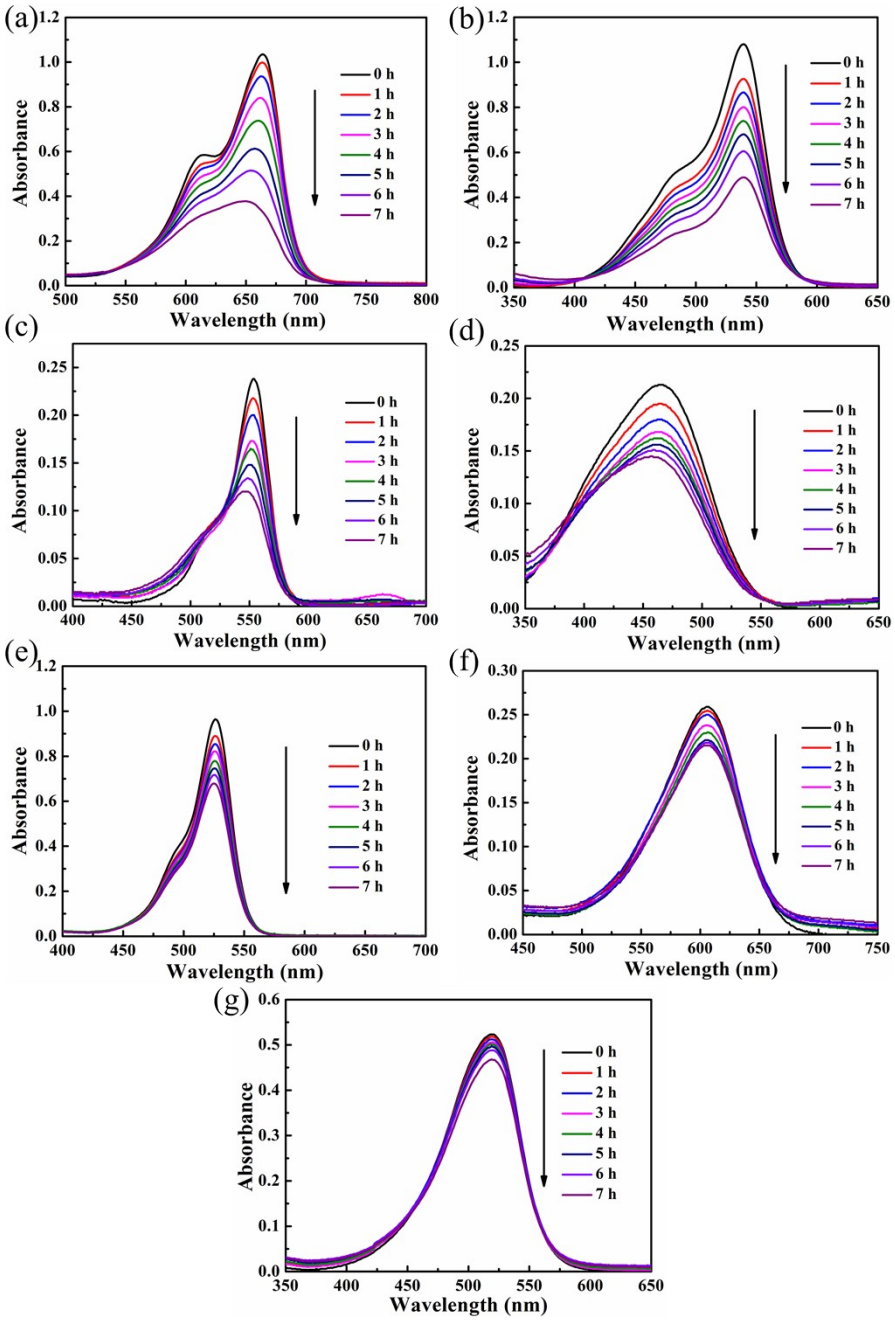

Fig. S15 Photocatalytic effects of compound **2** on different organic dye solutions: (a) MB, (b) PH, (c) RhB, (d) MO, (e) Rh 6G, (f) Isatin, (g) BR 2.

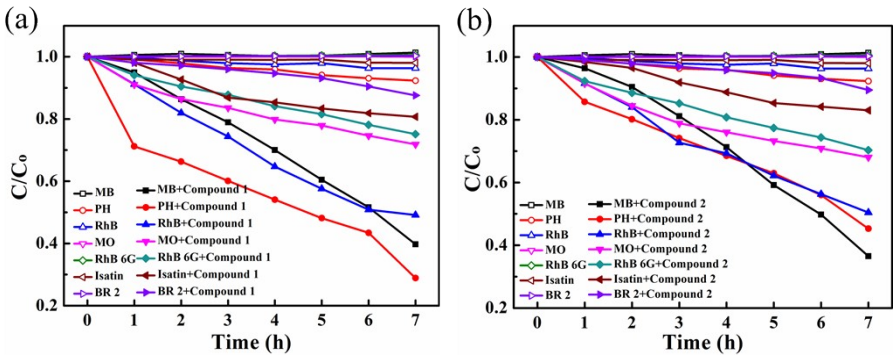

Fig. S16 The linear relation of concentration ratios (C/C_0) to irradiation time (h) for different organic dye solutions: (a) in the absence and presence of **1**; (b) in the absence and presence of **2**.

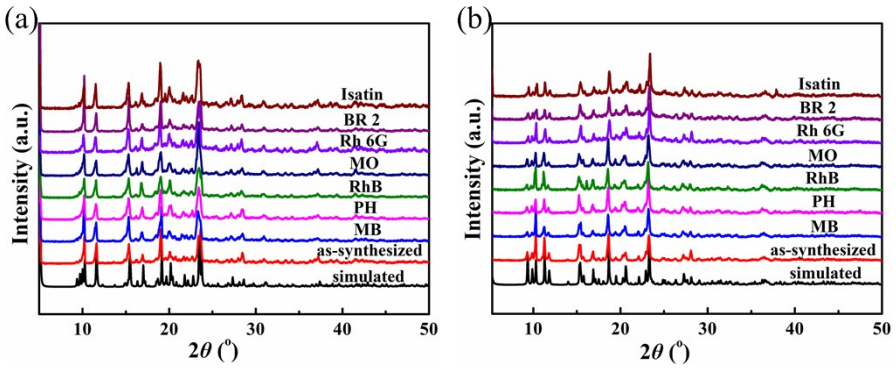

Fig. S17 (a) PXRD patterns of **1** after photocatalysis of different dyes. (b) PXRD patterns of **2** after photocatalysis of different dyes.

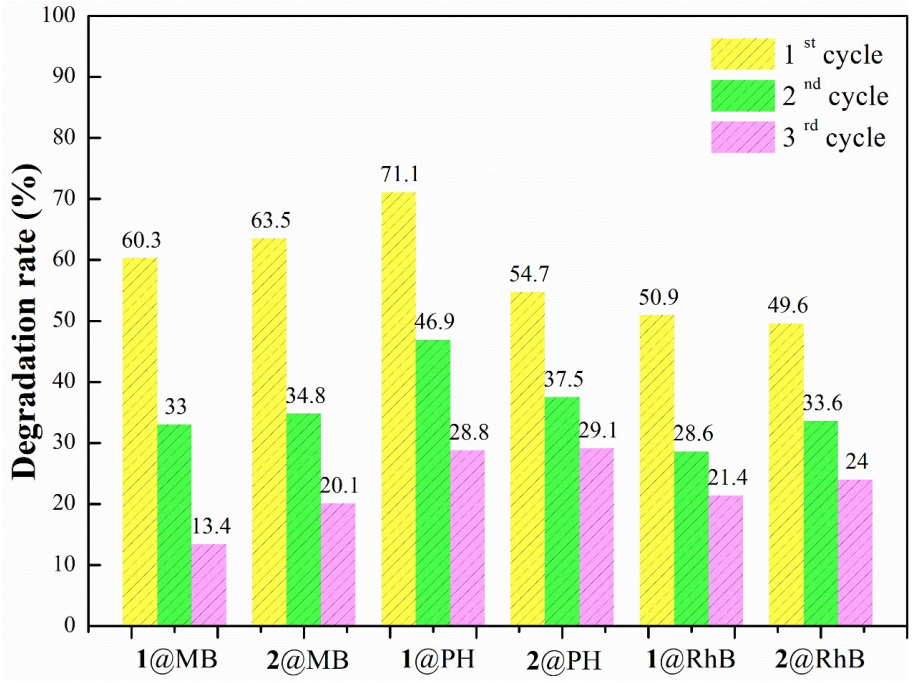

Fig. S18 Degradation rates of the MB, PH, RhB solutions in the presence of compounds **1** or **2** for three cycles.

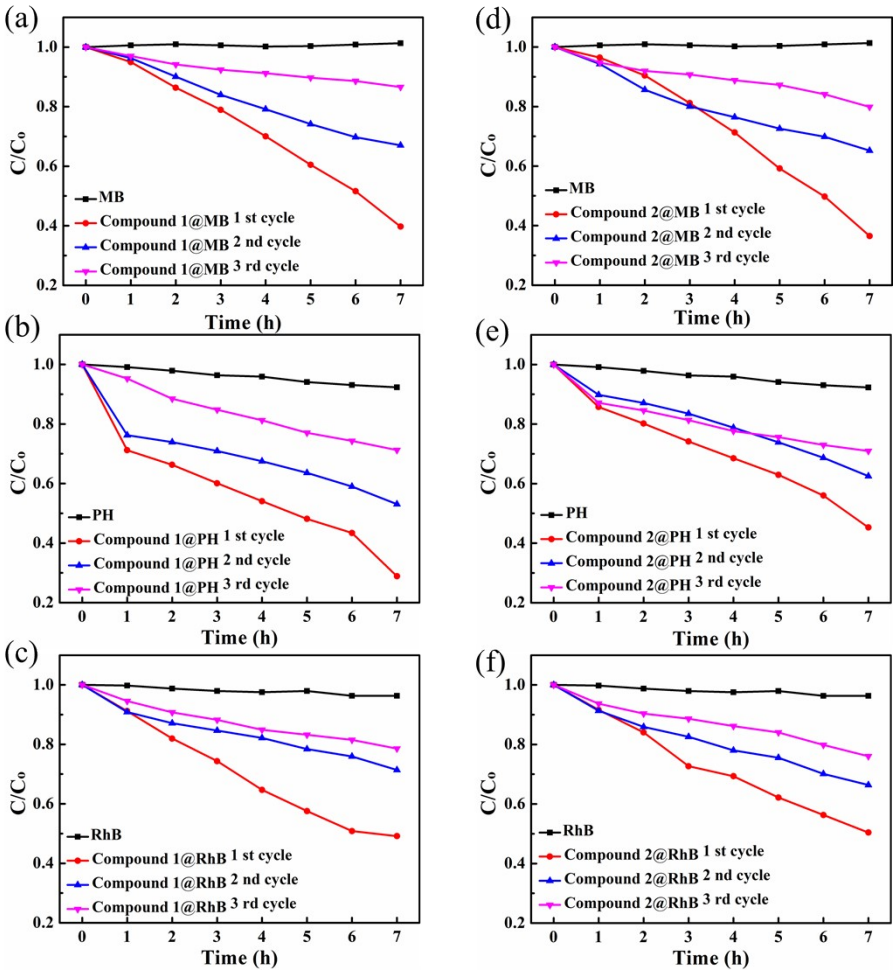

Fig. S19 The linear relation of concentration ratios (C/C_0) to irradiation time (h) for different organic dye solutions: (a) MB, (b) PH, (c) RhB in the absence and presence of **1** for three cycles; (d) MB, (e) PH, (f) RhB in the absence and presence of **2** for three cycles.

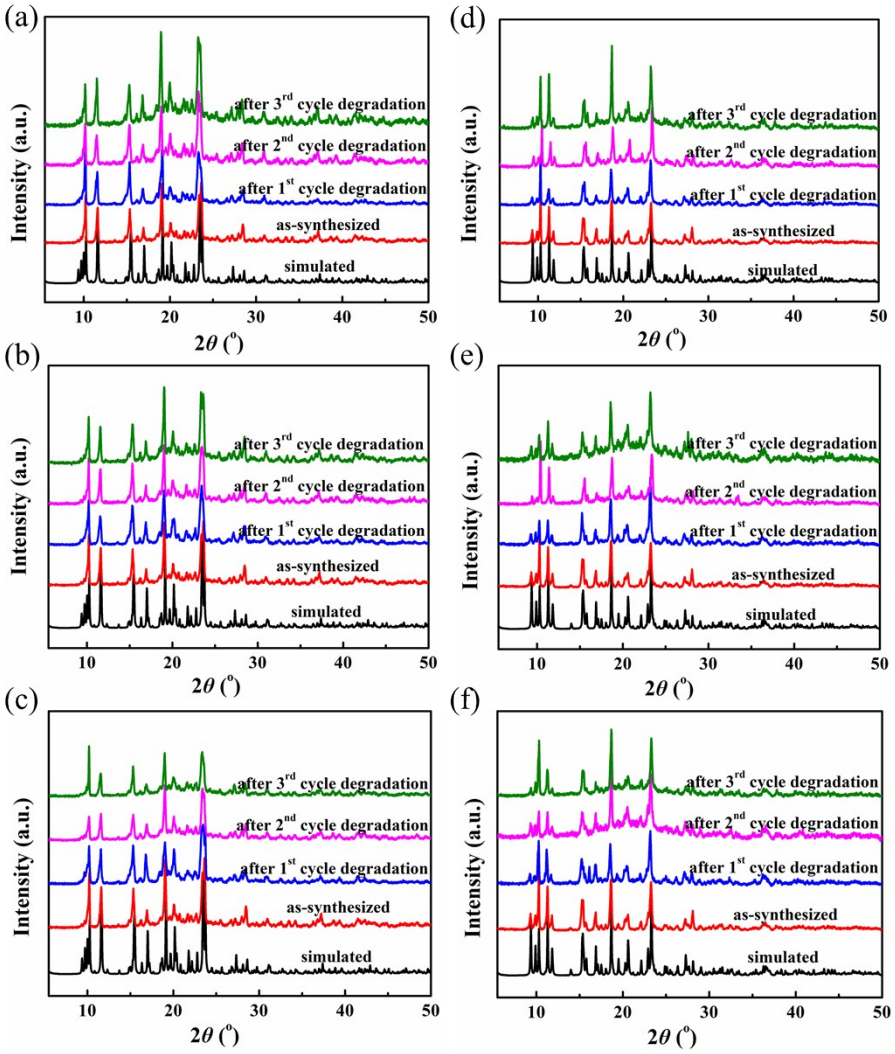

Fig. S20 PXRD patterns of **1** after photocatalysis of (a) MB, (b) PH, (c) RhB solutions and **2** after photocatalysis of (d) MB, (e) PH, (f) RhB solutions for three cycles.

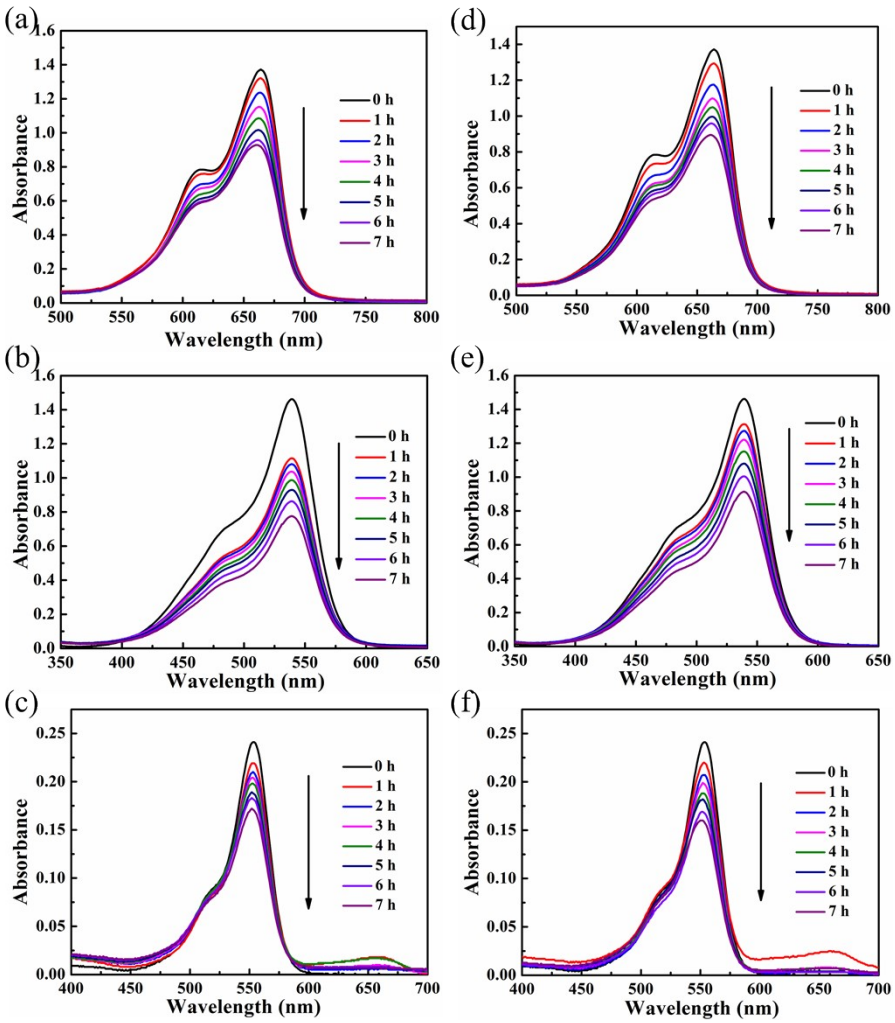

Fig. S21 Photocatalytic effects of **1** on (a) MB, (b) PH, (c) RhB solutions and **2** on (d) MB, (e) PH, (f) RhB solutions for second cycle.

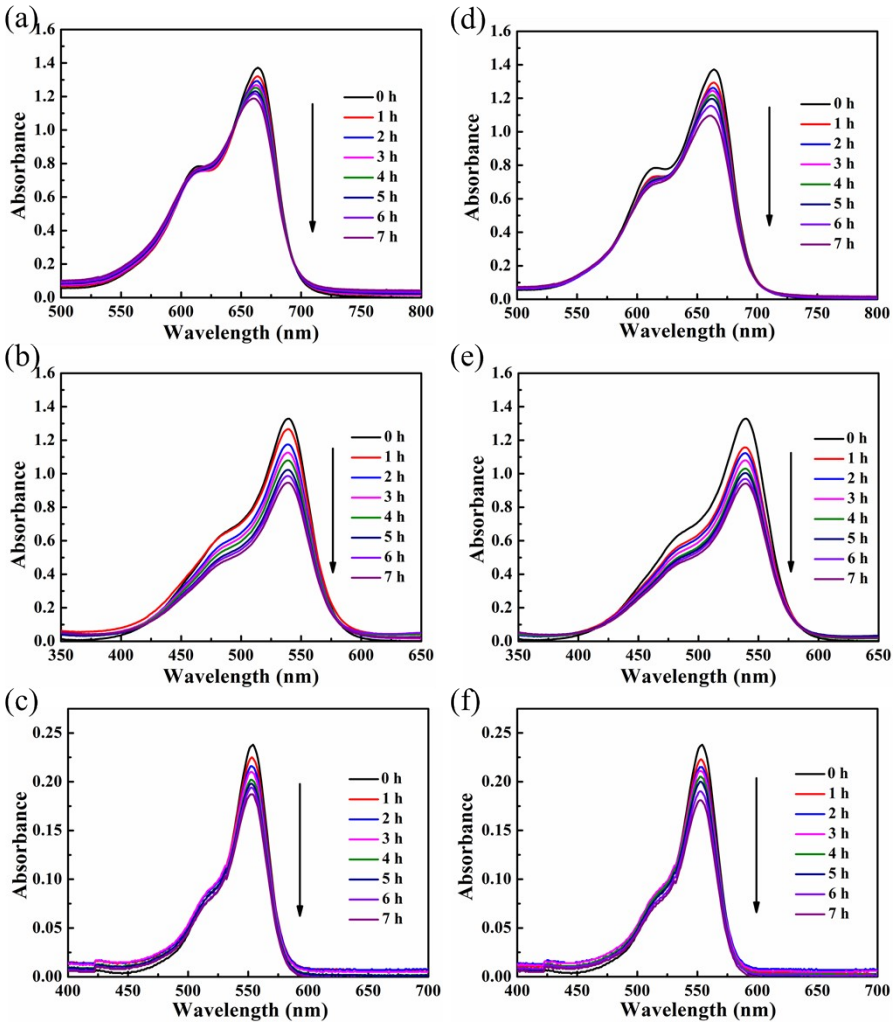

Fig. S22 Photocatalytic effects of **1** on (a) MB, (b) PH, (c) RhB solutions and **2** on (d) MB, (e) PH, (f) RhB solutions for third cycle.